Assessment of the planned demonstration site

Version 2

Deliverable 6.1

Christian Rod, Pierre-Jean Alet, Nelson Koch

21 February 2018

INTERNAL REFERENCE

- **Deliverable No.:** D 6.1
- **Deliverable Name:** Assessment of the planned demonstration site
- **Lead Partner:** CSEM
- **Work Package No.:** 6
- **Task No. & Name:** 6.1 Test bed implementation study dc grid
- **Document (File):** DCSMART_CRd_D6p1.docx
- **Issue (Save) Date:** 2018-02-21

DOCUMENT SENSITIVITY

☐	**Not Sensitive**	Contains only factual or background information; contains no new or additional analysis, recommendations or policy-relevant statements
☒	**Moderately Sensitive**	Contains some analysis or interpretation of results; contains no recommendations or policy-relevant statements
☐	**Sensitive**	Contains analysis or interpretation of results with policy-relevance and/or recommendations or policy-relevant statements
☐	**Highly Sensitive Confidential**	Contains significant analysis or interpretation of results with major policy-relevance or implications, contains extensive recommendations or policy-relevant statements, and/or contain policy-prescriptive statements. This sensitivity requires SB decision.

DOCUMENT STATUS

	Date	Person(s)	Organisation
Author(s)	31/01/2018	Christian Rod, Nelson Koch	CSEM
Verification by	21/02/2018	Pierre-Jean Alet	CSEM
Approval by			

CONTENTS

Disclaimer

The content and views expressed in this material are those of the authors and do not necessarily reflect the views or opinion of the ERA-Net SG+ initiative. Any reference given does not necessarily imply the endorsement by ERA-Net SG+.

About ERA-Net Smart Grids Plus

ERA-Net Smart Grids Plus is an initiative of 21 European countries and regions. The vision for Smart Grids in Europe is to create an electric power system that integrates renewable energies and enables flexible consumer and production technologies. This can help to shape an electricity grid with a high security of supply, coupled with low greenhouse gas emissions, at an affordable price. Our aim is to support the development of the technologies, market designs and customer adoptions that are necessary to reach this goal. The initiative is providing a hub for the collaboration of European member-states. It supports the coordination of funding partners, enabling joint funding of RDD projects. Beyond that ERA-Net SG+ builds up a knowledge community, involving key demo projects and experts from all over Europe, to organise the learning between projects and programs from the local level up to the European level.

www.eranet-smartgridsplus.eu

1. Context

DCSMART is an interdisciplinary project that aims at enabling a straightforward integration of smart grid system technologies, creation of market opportunities and stakeholder's adoption through the development and implementation of DC distribution smart grids.

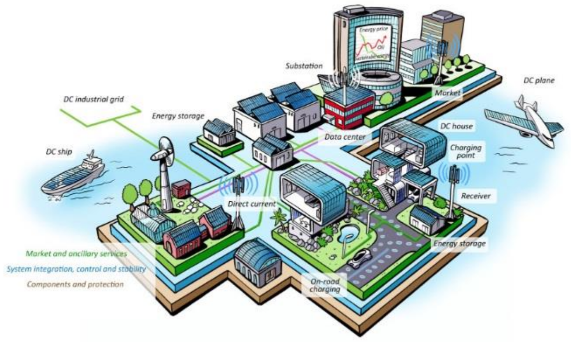

Figure 1: illustration of a smart DC distribution

It is funded through the ERA-NET Smart Grids Plus action and brings together partners from the Netherlands, Germany and Switzerland.

In this context CSEM is in charge of developing a demonstration microgrid able to emphasize the advantages of low-voltage DC distribution, local management of renewable energy sources (RES) and implementation of advanced control techniques with the ultimate objective of integrating RES as seamlessly as possible from both DSOs and final user points of view.

From the Swiss side, the DCSMART project involves the City of Neuchâtel and Viteos SA, the local DSO. The demonstration micro-grid will be installed in one of the building of Neuchâtel Water Treatment Plant (WTP).

2. Swiss demonstration site

2.1 Energy production and consumption at Neuchâtel WTP

The Water Treatment Plant (WTP) of Neuchâtel not only treats the waste water of the city and its neighbourhood (nearly 7 million cubic meters) but is also an important contributor to various local energy networks, mainly the medium voltage electrical grid and the local district heating.

Indeed, regarding the district heating, Neuchâtel WTP recently commissioned a Combined Heat and Power (CHP) unit. This unit valorises the biogas produced by the different biological and chemical processes of the water treatment. The produced heat (2.5 millions of kWh) and power (2 millions of kWh) are primarily destined to cover the WTP own needs, with the extra productions fed to the local grid and distributed to nearby consumers. Moreover, on the electrical side, most of the WTP rooftops are now covered with photovoltaic panels exploited by the local utility company, thus reinforcing the City commitment to the promotion of renewable energy sources.

From this point of view, the selection of this public premises to implement the Swiss demonstrator of a DC micro-grid takes all its sense. Indeed, the perspective of integrating innovative technologies to reduce the overall energy consumption and improve the energy efficiency fully integrate in this trend.

Figure 2 presents a complete overview of the energy production and consumption on this site.

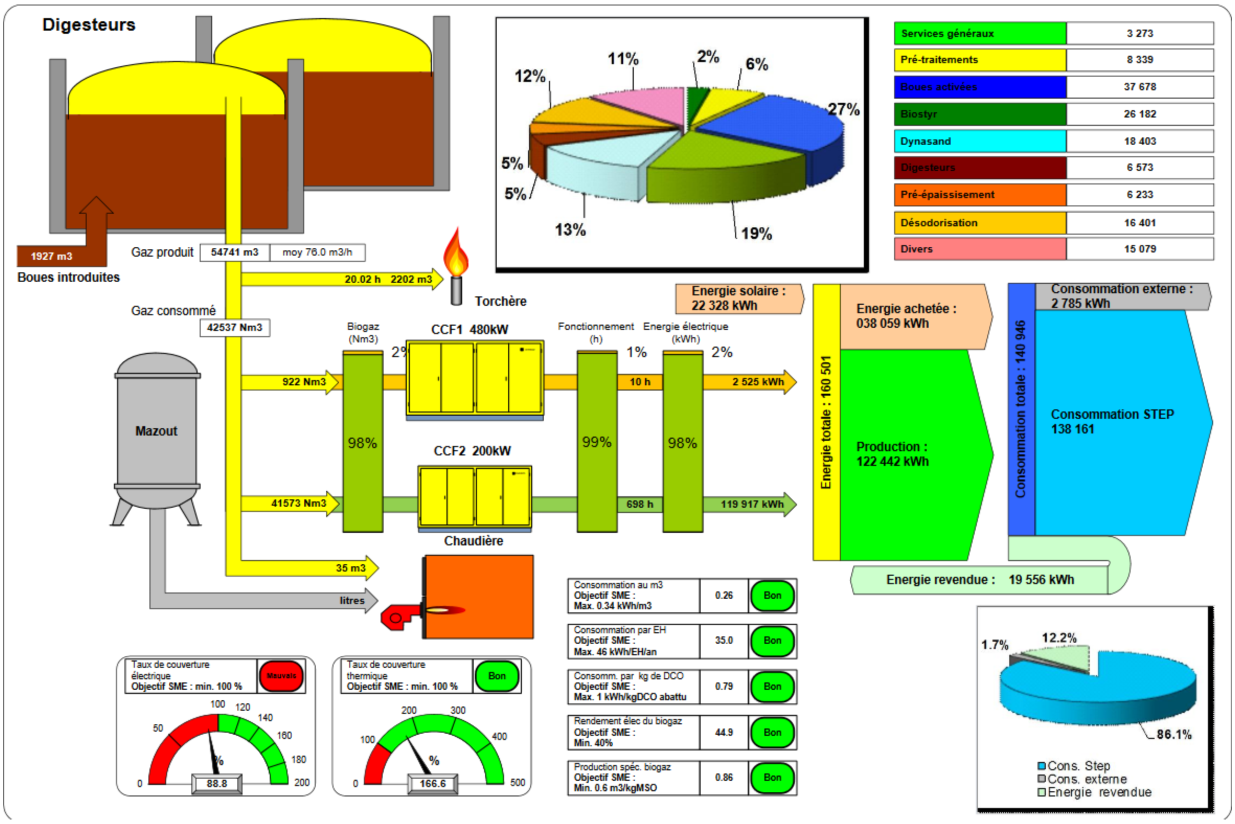

Figure 2: Overview of energy production and consumption on the Swiss demonstration site; source: Service des infrastructures de la Ville de Neuchâtel.

On-site electricity production currently comes from:

- Solar PV (181 MWh/yr)
- Biogaz CHP (1'540 MWh/yr)

On-site electricity consumption is 1'859 MWh/yr. The resulting self-sufficiency and self-consumption ratios are 78% and 84% respectively.

2.2 Target building

The initial goal of the Swiss Demonstration Site (SDS) was to improve the energy consumption of the administrative building of Neuchâtel WTP, especially through the installation of LED lighting and electrical heating and/or cooling systems, the intrinsic flexibility of which could be used to implement demand side management strategies.

However, after discussions with Neuchâtel WTP staff, it appeared that the considered building had already been recently equipped with such lighting systems. Moreover, the whole WTP site is connected to the district heating and the local free-cooling system, which eliminates the need for electrical heating or cooling.

Figure 3: Neuchâtel WTP with the administrative building (A) and the industrial one where the SDS will be installed (B). Source: Service des infrastructures de la Ville de Neuchâtel.

The decision has thus been taken to integrate the Swiss demonstrator into one of the industrial building of Neuchâtel WTP (Figure 3) where many processes, with significant electrical energy consumptions, are present, thus adding significance to the project results. Indeed, industrial installations present a far greater potential for technology transition due to the more important influence such customers can have on the market and the bigger diversity of the encountered applications.

2.3 Target loads: industrial motors

2.3.1 Existing motors on the plant

At the project beginning, it was planned to integrate in the demonstrator loads already in use in the industrial part of Neuchâtel WTP. These loads were frequency converters used to drive induction motor destined to applications such as ventilation or pumping.

Figure 4: Frequency converter initially selected for integration in the demonstrator

These frequency converters provide DC terminals, normally intended for plugging braking resistors. It was planned to use these same terminals to connect these frequency inverters to the developed micro-grid.

Nevertheless, test conducted on a spare device have shown that such a connection was not possible. Indeed, the voltage measured between the DC terminals seems to depend on the converter state, as schematized on Figure 5. More precisely, a near zero value has been measured with a stopped motor. This is most probably due to the presence of an internal transistor the purpose of which is to enable or disable the braking resistors.

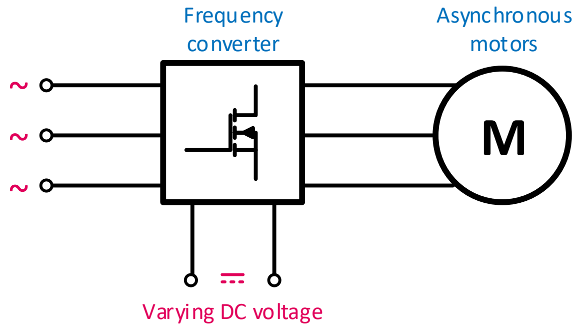

Figure 5: illustration of the varying voltage issue

An alternative solution consisting in supplying the frequency converter through the front-end diode rectifier, as illustrated on Figure 6, has been investigated.

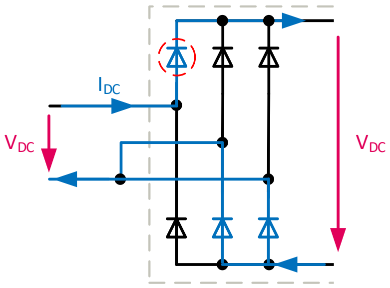

Figure 6: overheating issue cause by a DC supply through the rectifier

Even if this solution allows to solve the varying voltage issue, it introduces another one. Indeed, even if it is possible to connect two legs in parallel in order to split in two either the going or returning current, one of the diode will permanently carry the full current. This will introduce overheating issues since the cooling system has been designed in order to accommodate diodes conducting during only one third of the time.

Even if working from a functional point of view, this solution has been rejected due to the probable associated reliability issues that it would have raised and which are unacceptable in the context of a 24/7 exploitation.

Therefore, an alternative solution had to be developed, as described in section 3.3. This solution has been designed to replicate the consumption behaviour of the loads in use at Neuchâtel WTP, allowing to exploit the results almost as if the measurements had been taken on the real system.

2.3.2 Energy consumption

Figure 7 illustrates a typical week of consumption of one the ventilation unit of Neuchâtel WTP. The time origins corresponds to 7 am of the first recorded day.

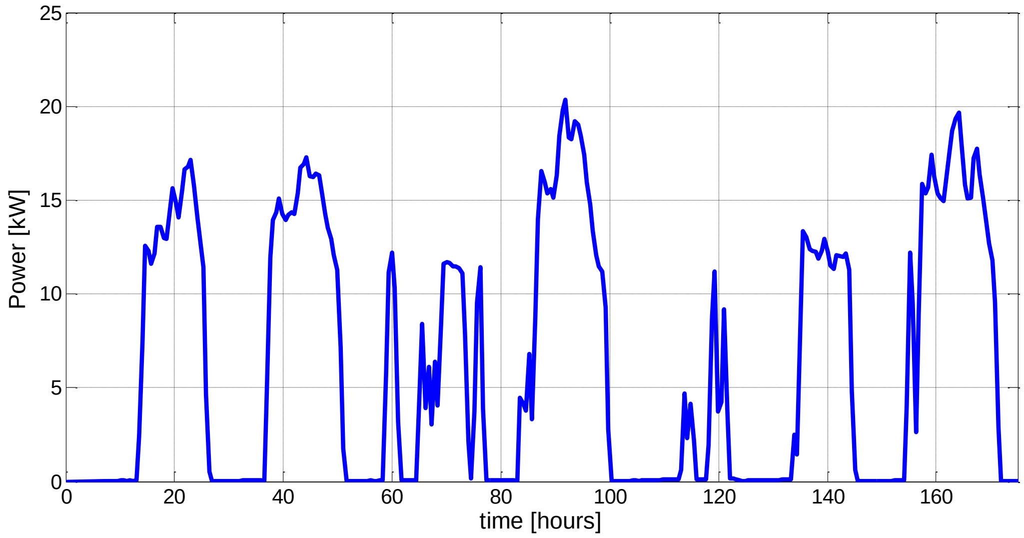

Figure 7: Consumption profile of the ventilation unit of Neuchâtel WTP

This consumption profile clearly shows a daily pattern, characterized by important peaks and a consumption going down to zero. One can also observe that the peaks occur at night and are therefore not aligned with the PV production.

From these observation, it seems that applications with such power profiles could greatly benefit from the increased self-consumption and peak-shaving services that the DCSMART approach could provide.

2.4 Photovoltaic production

Based on the remaining available space on WTP rooftops and discussions with the people managing Neuchâtel WTP, a photovoltaic system with a rated power of 10 kWp has been agreed upon. This power rating corresponds to a trade-off between budget constraints and the needs of the developed DC micro-grid and those of Neuchâtel WTP. Indeed, it is currently planned to integrate the photovoltaic installation in the low-voltage AC grid of Neuchâtel WTP at the project completion.

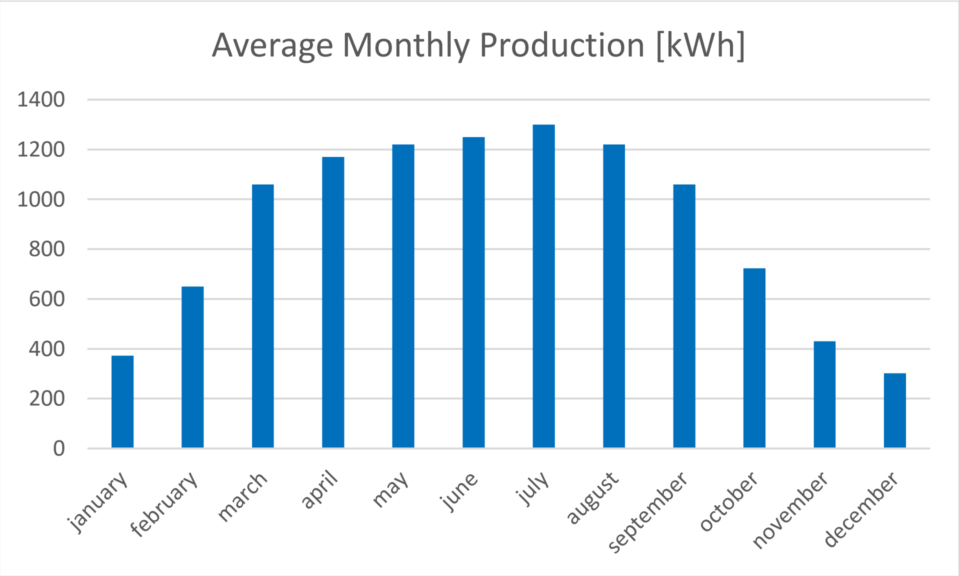

Figure 8: Production estimation for the considered system

Figure 8 shows an estimation, as calculated with PV-GIS,[1] of the monthly production based on parameters presented in Table 1. The system inclination (angle relative to the horizontal plane) and orientation (angle relative to the direction of the South) corresponds to optimal parameters computed by the prevision tools based on the system location. The estimated losses include the losses related to the temperature and the low irradiance, the angular reflectance effects and the electrical losses.

Table 1: Parameters of the considered photovoltaic system

Rated power	Inclination	Orientation
10 kWp	35 °	-1°
Position	**Technology**	**Estimated total losses**
46°59'39" N, 6°56'49" E	Crystalline silicon	23.5 %

A yearly average production of approximately 10'800 kWh is expected. Such a production corresponds respectively to approximatively 24%, 65% and 150% of the yearly consumption of the typical profiles defined under 3.5.1.

3. Structure of the demonstrator

3.1 Additional services for DSO and final users

At the beginning of the project, it was planned to upscale, from a table-top demonstrator to a full size system, the application of the previously developed control strategy,[2] the main goal of which was to improve the quality of the power exchanged with the AC distribution grid by reducing its variability. This approach is known as ramp-rate control.

Even if its contribution to grid stability can be particularly significant in weak grids such as those that can be found in developing countries, the power variability doesn't have consequences of such importance in the strong and stable European grids.

For this reason, additional services have been included in the control strategy that will be implemented in the Swiss demonstration site: the limitation of the exchanged power, known as peak shaving, and the increase of the local consumption of the locally produced energy, also named increased self-consumption. These services benefit both DSOs and final users.

Indeed, costs of distribution grids are mainly linked to their rated power and only marginally to the transiting energy. For this reason, curtailment is more and more often mentioned as a solution allowing to increase the RES penetration, like in Germany where a limitation to 70% of the rated power of PV installations is mandatory.[3]

---

[1] http://re.jrc.ec.europa.eu/pvgis/

[2] Vincenzo Musolino and others, 'Alleviating Power Quality Issues When Integrating PV into Built Areas: Design and Control of DC Microgrids', in *IEEE First International Conference on DC Microgrids* (presented at the IEEE first international conference on DC microgrids, Atlanta, GA, USA, 2015), 102–7.

[3] J. von Appen and others, 'Time in the Sun: The Challenge of High PV Penetration in the German Electric Grid', *IEEE Power and Energy Magazine*, 11/2 (2013), 55–64.

For the same reason and due to the emergence of prosumers, DSOs are currently expressing a will to charge the energy distribution based also on the maximum exchanged power and not only on the consumed energy anymore.[4]

Thus, it can be interesting for final users whose energy consumption shows important power peaks to be equipped with a system allowing to reduce this maximum exchanged power while ensuring the correct operation of their different appliances.

Finally, because of decreasing incentives for energy injection in the distribution grid, local consumption of energy produced by distributed RES is more and more interesting for the final user. If this consumption is not aligned with the production, an energy storage system with an appropriate control strategy is needed.

3.2 General topology

The studied system is schematically represented on Figure 9.

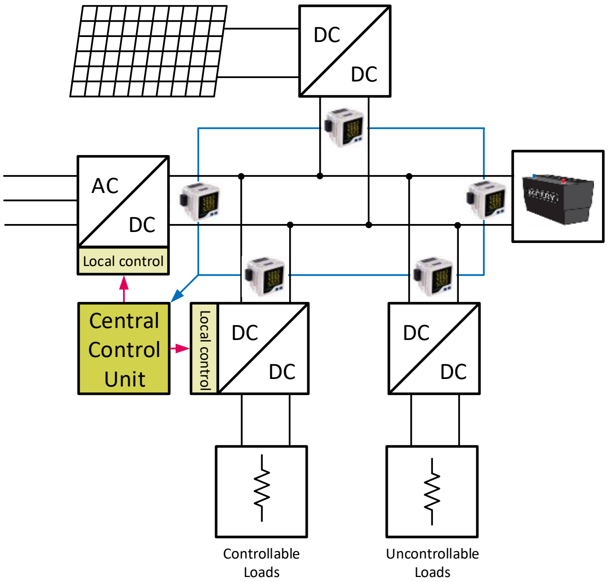

Figure 9: General topology of the Swiss Demonstrator

3.2.1 Main components

This system is composed of the following elements:

- A single bidirectional AC/DC converter the role of which is to interface the DC micro-grid with the upstream AC low voltage distribution grid. This converter is linked to a local controller in order to compute voltage, current, and power set-points. The DC side of this grid-tied converter is the common DC-link to which all the micro-grid elements are connected.
- A photovoltaic system, represented by a PV module and its DC/DC power optimizer.
- A central control unit, the roles of which are the system supervision and the transmission of set-points to the different local controllers.
- DC/DC converters, supplying both the flexible and the standard loads with adequate voltages. The converter dedicated to the flexible loads is directly linked to a local controller.

[4] A. Van den Bossche, B. Meersman and L. Vandevelde, 'Fundamental Tarification of Electricity', in *2009 13th European Conference on Power Electronics and Applications*, 2009, 1–7.

- A directly-connected energy storage system, here represented by a battery even if the exact nature of this element has not been finalized yet. The fact that this ESS is directly connected imposes to the main DC-link a voltage varying with its State of Charge (SoC). This varying voltage allows all the connected element to have a direct access to this fundamental information, thus allowing to massively reduce the required communication infrastructure. This approach is known as DC-bus signaling.[5]
- Smart-meters are connected to each of the different feeders. Their measurements are gathered and stored in the central control unit.

Figure 10: Swiss Demonstrator Main cabinet

Figure 10 illustrates the main cabinet of the SDS, which contains the grid-tied AC/DC converter, the protection system, and local and central control units and the various smart-meters. The stabilizing DC/DC converters will soon be integrated in it. Another cabinet, hosting the energy storage system, is planned to be added to this one.

3.2.2 Power flows

Figure 11 graphically defines the different power flows occurring in the system depicted on Figure 9. Blue and red arrows respectively define positive and negative flows for the different elements according to the sign convention used in this document.

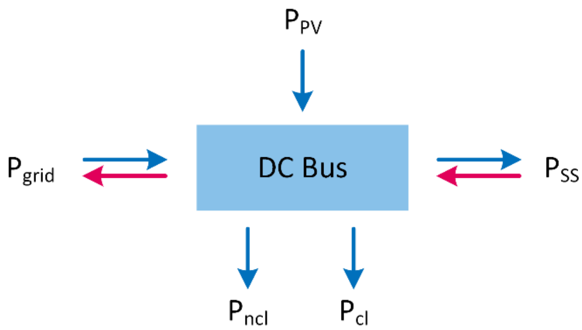

Figure 11: Definition of power flows

Thus, the internal power balance P_{bal} is defined according to the following equation:

---

[5] J. Schonbergerschonberger, R. Duke and S. D. Round, 'DC-Bus Signaling: A Distributed Control Strategy for a Hybrid Renewable Nanogrid', *IEEE Transactions on Industrial Electronics*, 53/5 (2006), 1453–60.

$$P_{bal} = P_{PV} - P_{ncl} - P_{cl} \qquad (1)$$

Therefore, a positive power balance means a local production larger than the local consumption. In such a case, the excess production is either stored in the ESS or rejected to the upstream AC distribution grid.

On the other hand, a negative power balance means that the local consumption exceeds the local production. In such cases, the required additional power is provided either by the distribution grid, through the interface AC/DC converter, or by the Energy Storage System, depending on its SoC, as further explained in chapter 4.

3.3 Purpose-built load system

As explained in details in chapter 2, the initially planned loads from WTP have proved to be incompatible with the developed demonstrator. Nevertheless, a system aiming at replicating their energy consumption has been developed. This system is illustrated on Figure 12.

Figure 12: Purpose-built load system of industrial motors

This system is composed of three distinct subsystems made of DC/AC converters, brushless DC motors and magnetic powder breakers supplied by a common insulated DC/DC converter, mandatory to stabilize the applied DC voltage and due to the grounding of the return wire of the common DC-link.

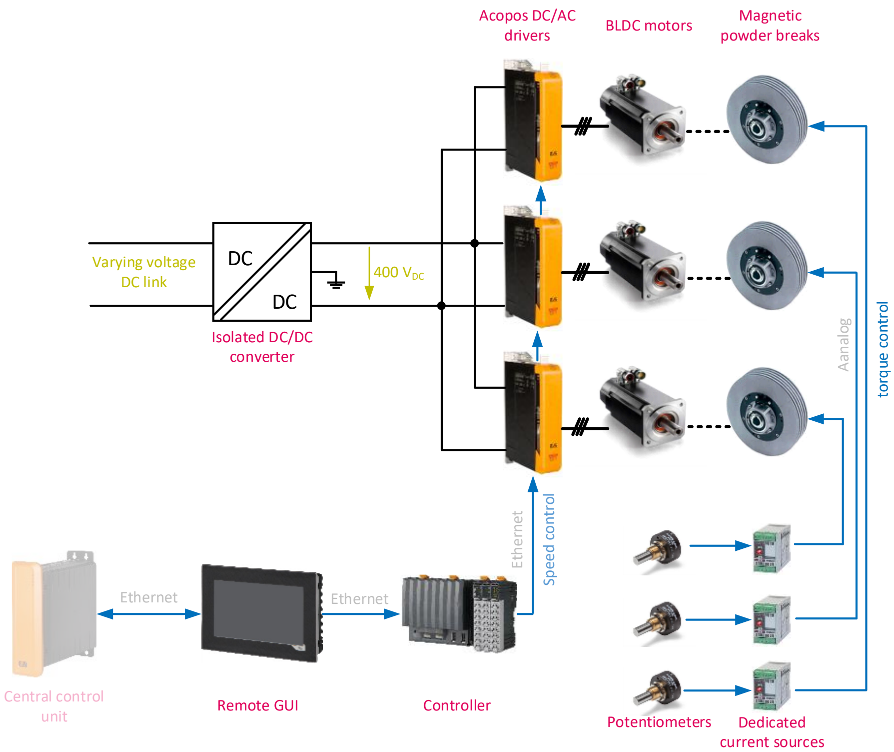

Figure 13: Components of the purpose-built load system

Speed cycles can be defined on a remote graphical interface that can eventually be duplicated on the central control unit. These speed cycles are then processed in a PLC that ensure the speed control of the motors through an internet communication with the DC/AC inverters. Finally, potentiometers linked to dedicated current sources allow to control the resistive torque applied to the magnetic breaks that are cooled by fans that are not represented.

3.4 Bill of material

Since finding compatible devices may be an important issue when developing DC distribution systems, a summary of the most important pieces of equipment is given is this section, under the form of Table 2. A short description of each component is given after this table.

Table 2: Bill of main pieces of equipment

#	Device/Function	Manufacturer	Reference
1	Controllable AC/DC converter	Regatron	TopCon TC.GSS
2	DC smart meters	Accuenergy	Acu243
3	DC differential protection relays	Dossena	DER3BDUAL/6D
4	DC circuit breakers	ABB	S802PV
5	Controllable drives with DC inputs	B&R automation	8EI8X8HWS10.0600-1
6	DC/DC string optimizer	AMPT	V750 13.5

1. **Controllable AC/DC converter:** This bidirectional AC/DC converter is able to supply a positive DC voltage (up to 600V) with a positive or negative current. It can operate either in constant voltage, constant current or constant power modes. Moreover, it can be controlled by many interfaces, the simplest one being a set of digital and analogue inputs.
2. **DC smart meter:** These meters are equipped with a RS-485 communication interface that allow them to be easily integrated in a larger system. Moreover, they provide a lot of advanced measurements such as the total drawn or injected energy. The used model uses direct voltage sensing and remote hall-sensors for current sensing.
3. **DC differential protection relays:** These differential protection relays use remote current sensing hall sensors to provide a protection against accidental grounding.
4. **DC circuit breakers**: These breakers are standard industrial ones, mainly used in photovoltaic installations.
5. **Controllable drives with DC inputs**: these drives, used in conjunction with B&R automation motors, provide DC terminals alongside the classical AC ones. These terminals are nominally used to parallel different motors in order to feed the breaking energy of the decelerating ones to the other ones, the rectifier stage being a diode bridge. In the case of the Swiss Demonstrator, these terminals are directly connected to a stabilized DC voltage provided by an insulated DC/DC converter fed by the general DC-link.
6. **DC/DC string optimizers**: These optimizers have been selected here for their ability to work with varying voltage on the DC-link stage.

3.5 Power consumption profiles

3.5.1 Scenario definition

Independently of the real power consumption profiles measured on loads in use at Neuchâtel WTP, three characteristic consumption profiles have been defined in order to assess the advantages of the developed solution in different cases.

These profiles are realized by adjusting the different parameters of the speed cycles of each of the three axis. These parameters are defined according to Figure 14. Each of them can be configured independently.

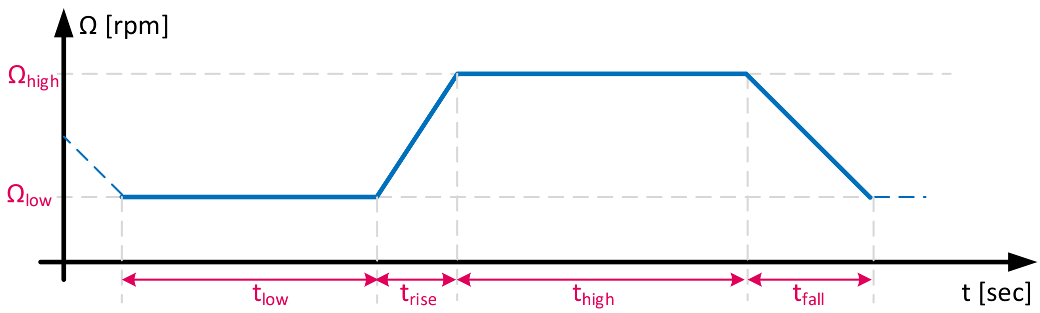

Figure 14: Definition of the speed cycles parameters

3.5.2 Low-variations scenario

The power profile associated with the first of the three scenarios is illustrated on Figure 15. The profile seen by the billing measurement devices, based on a moving average with a 15-minute resolution, is also represented.

It is characterized by relatively small and slow power variations. The underlying goal is to have a negligible power-related cost component.

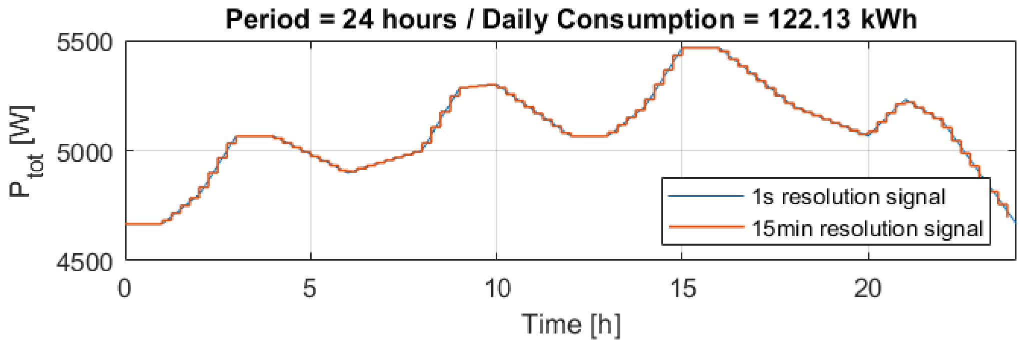

Figure 15: Power profile of the first scenario

The different drives must be configured according to Table 3 in order to obtain such a consumption profile.

Table 3: Drive configuration for the first scenario

Drive	Ωlow [rpm]	Ωhigh [rpm]	Tlow [s]	Thigh [s]	Trise [s]	Tfall [s]	Torque [%]
1	1000	1300	14400	21600	28800	21600	100
2	1300	1400	3600	21600	3600	14400	100
3	1200	1400	7200	3600	3600	7200	100

3.5.3 Medium-variation scenario

The power profile associated with the second scenario is illustrated on Figure 16. The power variations are more important than in the case of the first scenario. Nevertheless, a minimal consumption is always guaranteed, ensuring an intermediate repartition between the associated energy-based and power-based components of the costs.

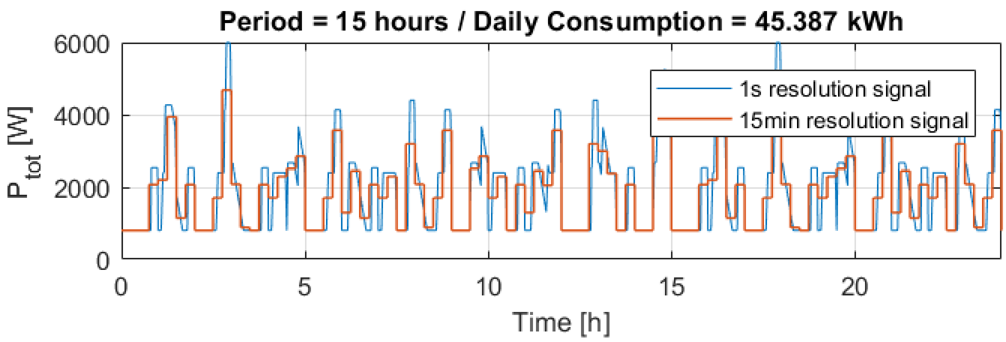

Figure 16: Power profile of the second scenario

The associated drive parameters are given in Table 4.

Table 4: Drives configuration for the second scenario

Drive	Ωlow [rpm]	Ωhigh [rpm]	Tlow [s]	Thigh [s]	Trise [s]	Tfall [s]	Torque [%]
1	200	1500	2880	600	60	60	100

Drive	Ωlow [rpm]	Ωhigh [rpm]	Tlow [s]	Thigh [s]	Trise [s]	Tfall [s]	Torque [%]
2	100	1500	4200	600	120	1080	100
3	300	1500	3900	1200	180	120	100

3.5.4 High-variation scenario

The power profile associated to the third scenario is illustrated below on Figure 17. This third scenario is characterized by a comparatively low energy consumption and important power spikes in order to obtain a dominant power-related cost component.

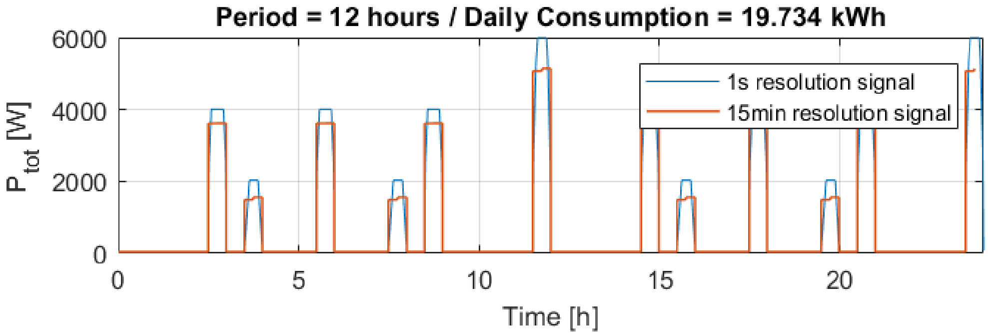

Figure 17: Power profile of the third scenario

The associated drive parameters are given in Table 5.

Table 5: Drives configuration for the third scenario

Drive	Ωlow [rpm]	Ωhigh [rpm]	Tlow [s]	Thigh [s]	Trise [s]	Tfall [s]	Torque [%]
1	10	1500	9000	1200	300	300	100
2	10	1500	9000	1680	60	60	100
3	10	1500	12600	900	480	420	100

4. Control strategy and sizing methodology

This chapter is dedicated to the micro-grid control strategy. First, its implementation, based on a multi-level approach, is described. Then, the way a single energy storage is used to provide different services is detailed. Finally, a methodology to size this ESS according to predefined objectives is described.

4.1 Implementation

4.1.1 General topology

Figure 18 illustrates the topology of the implemented control strategy that is split in three different levels: the physical system, the first control level characterized by fast and simple controllers, and the supervision level where more advanced and slower control technics are used. More details about these levels are given below.

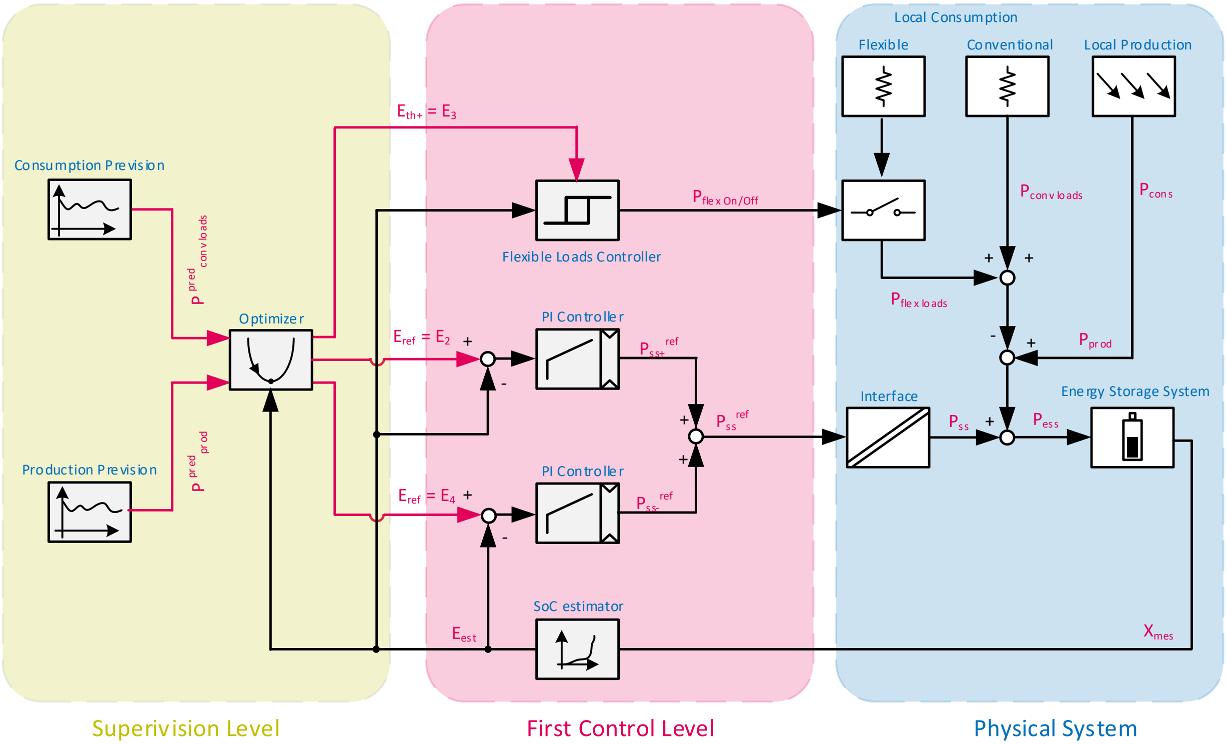

Figure 18: Layers and detailed implementation of the control strategy

On the lowermost level, the physical system, and as previously mentioned, the active and controllable elements are the AC/DC interface converter and the DC/DC converter supplying the flexible loads, here represented as a switch. The first one acts on the system by extracting power from of injecting power to the grid while the second can turn on or off the controllable loads.

These devices act on information coming from the first control level. There, the state of the complete system i.e. the SoC of the energy storage system, is estimated based on the DC-link voltage, assuming a bijective function linking these two values. This estimated SoC is compared to reference values to compute the error signal of two PI controllers the role of which is respectively to define the set-point for the power extracted from or injected into the AC grid. This estimation of the SoC is also compared to a third reference value in order to determine the state of the flexible loads.

These reference values can be fixed and predefined, during the system design for example, or continuously optimized based on previsions of the local production and consumption. These operations would occur at the supervision level.

4.2 Virtual splitting of the storage capacity

These considerations on the link between the different energy services and the parts of the energy storage capacity they use can be summarized according to Figure 19.

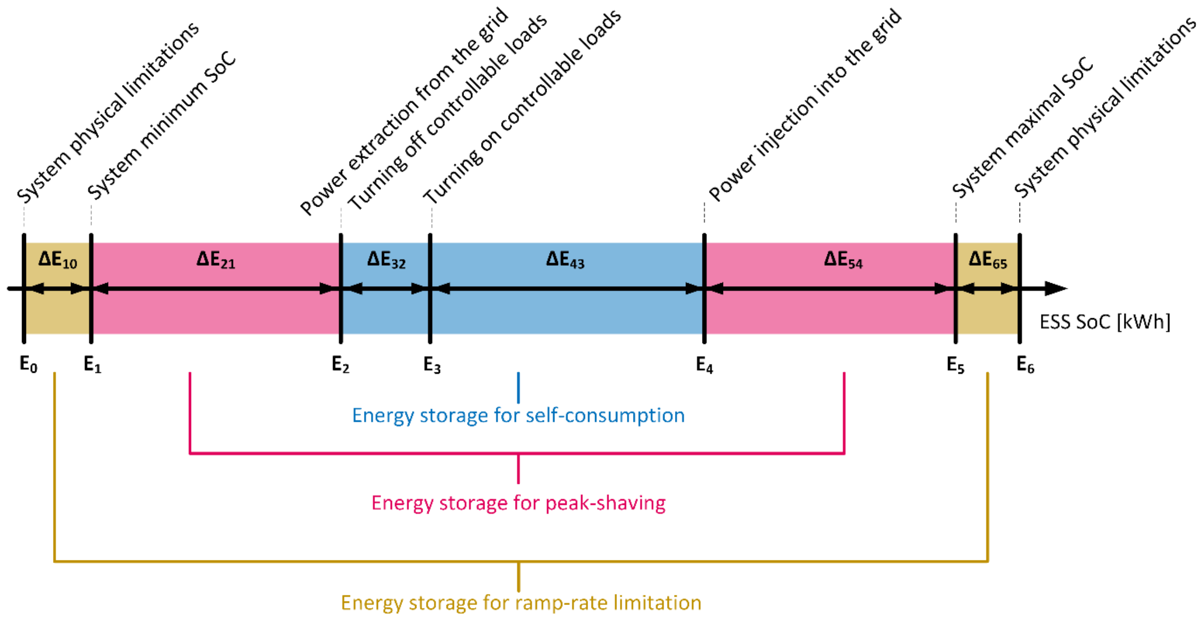

Figure 19: Repartition of storage capacity for the different services

The coloured areas correspond to the different energy services: yellow for the ramp-rate control, red for the peak-shaving and blue for the increased self-consumption. This last area includes an additional threshold, E_3, linked to the use of flexible loads. If the SoC reaches this value, the flexible loads will be turned on in order to increase the local consumption in order to bring the SoC back to E_2. In order to avoid ringing phenomena, a hysteresis is introduced and these flexible loads will not be turned off before the SoC reaches the lower bound of the area dedicated to self-consumption, namely E_2.

It must also be noted that ramp-rate limitation is also performed in the red areas. This detail is not mentioned on Figure 19 for the sake of simplicity.

4.3 Energy storage sizing tool

The control strategy being clearly defined, the behaviour of the closed-loop system can be studied in order to assess the energy storage capacity required to reach predefined objectives. This section is organized according to the different services provided by the micro-grid, namely the increased self-consumption, the ramp-rate alleviation and the peak-shaving.

4.3.1 Control of flexible loads for increased self-consumption

As can be seen on Figure 19, SoC thresholds can be introduced to control flexible loads in order to increase the self-consumption. Here, the flexible loads are turned on during periods of excess production, when the SoC reaches a predefined value E3 and turned off when the SoC reaches a level corresponding to the lower limit of the capacity dedicated to increased self-consumption. A hysteresis, noted ΔE_{32}, is introduced in order to avoid oscillations between the two modes.

This sizing methodology of this thresholds difference obeys to load-related constrains about minimal allowed cycle periods.

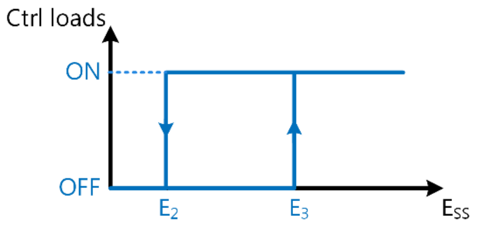

Figure 20: Hysteresis for the control of the flexible loads

Under the hypothesis of a constant power balance during the considered period, it can be mathematically demonstrated that the minimal time T_{min} separating the passage by the two thresholds can be expressed, in seconds, by the following equation, where ΔE_{32} is expressed in kWh and P_{cl} is the rated power, in W, of the controllable loads.

$$T_{min} = \frac{4 * \Delta E_{32} * 3.6 * 10^6}{P_{cl}} \quad (1)$$

Thus, from the controllable loads specifications, the hysteresis value can be computed in order to ensure a minimal on or off time.

4.3.2 Ramp-rate control

The yellow areas of Figure 19, dedicated to ramp-rate control, have to be considered as security margins against SoC overshoots due to perturbations on the power balance and the limited bandwidth of the PI controllers, as illustrated on Figure 21.

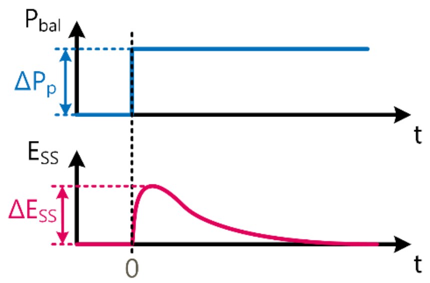

Figure 21: SoC overshoot due to perturbations

The sizing of ΔE_{10} and ΔE_{65} is based on a worst case scenario. An infinitely fast change of the power balance of a magnitude ΔP_p is considered. Then, from the system closed-loop transfer function and an inverse Laplace transform, it is possible to analytically express the time evolution of the stored energy as follows, where A and B are coefficients related to the closed-loop equivalent time constant and s_1 and s_2 the associated poles.

$$E_{ss}(t) = (A * e^{s_1 t} + B * e^{s_2 t}) * \Delta P_p + E_{ss}(t = 0) \quad (2)$$

The maximum value of E_{ss} is reached at $t=t_{max}$, given by the following equation.

$$t_{max} = \frac{\ln(s_1) - \ln(s_2)}{s_1 - s_2} \quad (3)$$

Thus, the energy overshoot ΔE_{ss} is defined as:

$$\Delta E_{ss} = (A * e^{s_1 t_{max}} + B * e^{s_2 t_{max}}) * \Delta P_p \quad (4)$$

Intervals ΔE_{10} and ΔE_{65} are sized to ensure that, in case of a perturbation of a magnitude ΔP_p, here selected as half the operating range, the energy stored in the storage system never exceeds the operating range.

4.3.3 Self-consumption and peak-shaving

By opposition to the two previously mentioned cases, the overall system behaviour cannot be studied analytically. Therefore, the sizing of the remaining intervals, namely ΔE_{21}, ΔE_{43}, and ΔE_{54}, is achieved through model-based simulations, as illustrated on Figure 22.

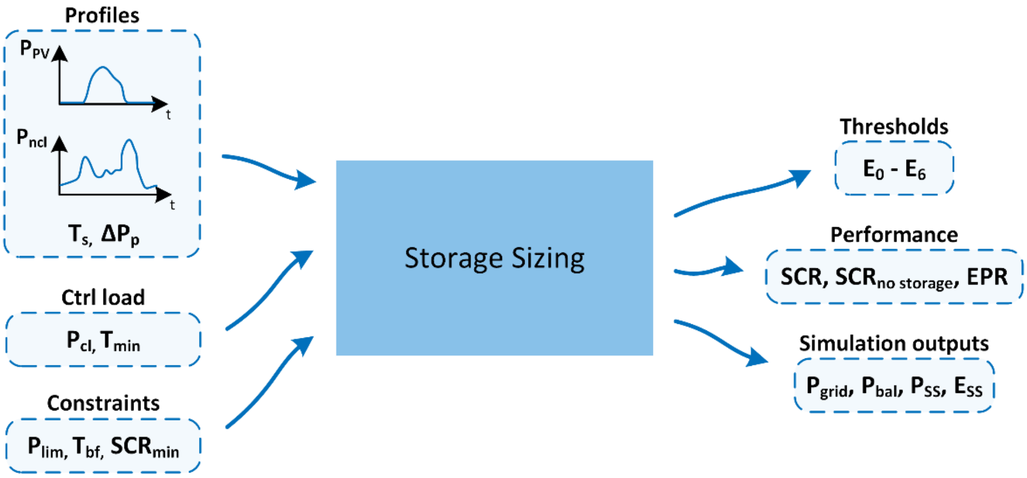

Figure 22: Working principle of the ESS sizing tool

Production and consumption profiles are fed to the model, alongside parameters such as the rated power of the flexible loads and the associated minimal cycle period and constraints linked to the performances objectives, such as the power limitation, the closed-loop equivalent time constant defining the ramp-rate alleviation and the minimal acceptable self-consumption ratio SCR_{min}.

The control thresholds E_0 to E_6 are then iteratively adjusted until the specified performances are met. The achieved self-consumption ratio is compared to the one that would have been achieved in the absence of any energy storage system. The Energy to Power Ratio (EPR) is also computed in order to determine the most suitable energy storage technology. Finally, the different relevant power profiles are computed for representation purposes.

4.3.4 Simulation results

Illustrations of the model and sizing tool possible outcomes are given in this section. Figure 23 shows the results of a day simulation using a reference balance power profile P_{bal}. The related simulation parameters and sizing objectives are summarized in Table 6.

Table 6: Simulation parameters

Maximal perturbation	**Flex. loads rated power**	**Flex. load min. cycle time**
ΔPp = 10 kW	Pcl = 1 kW	Tmin = 10 minutes
Grid power limitations	**Min. self-consumption**	**Ramp-rate control equivalent time**
Pmax = 5 kW	SCRmin = 70%	Tbf = 30 sec

The upper part of Figure 23 shows the day profile of the power exchanged with the upstream AC grid. One can observe both the reduction of the time variations and the respect of the maximal injection and extraction values P_{lim}^{ext} and P_{lim}^{inj}.

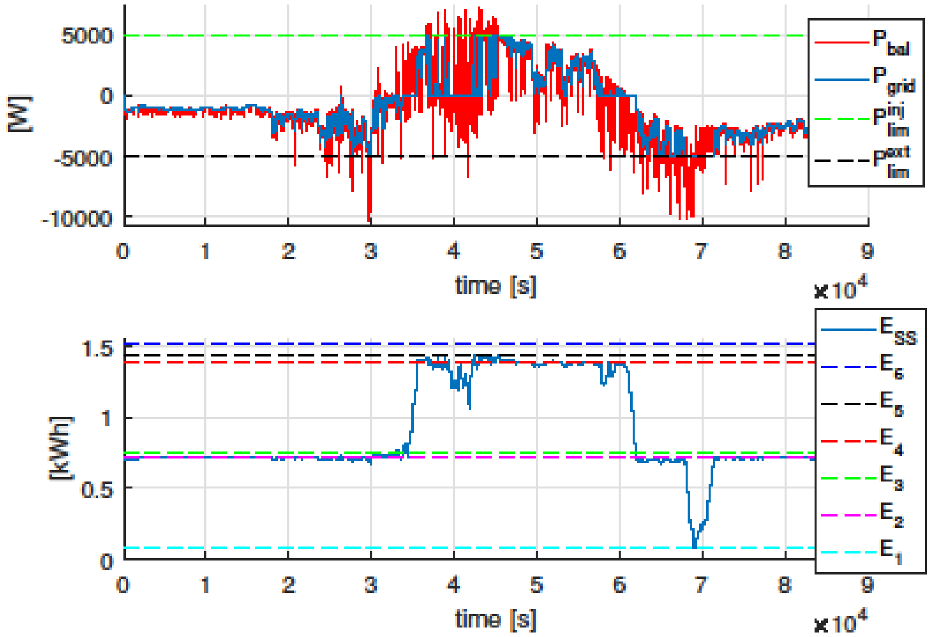

Figure 23: Power and ESS SoC profiles

The lower part of the same figure shows the corresponding evolution of the energy stored in the ESS. The computed control thresholds are represented on Figure 24 in reference to Figure 19.

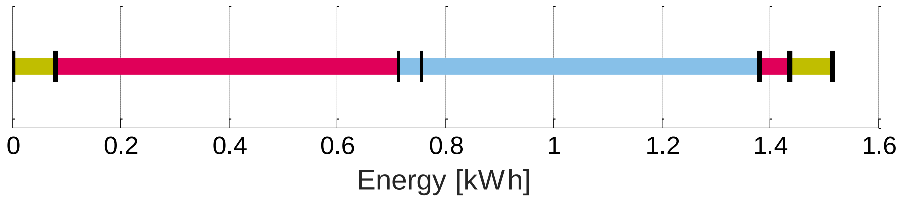

Figure 24: Sizing tool results

5. Economic assessment

Besides technical considerations, the economic impact of the system is also evaluated. Tools have been developed allowing an accurate economical assessment based on currently used billing rates. Three different analyses are performed. First, the impact of the energy and power tariff on the economic performance is assessed. Then, the effect of the levelized cost of storage (LCOS), which account for the cost of the storage system and its lifespan, is evaluated. Finally, an evaluation of the impact of the load profile shape is performed based on the reference profiles defined in 3.5.1.

5.1 Case study definition

The analysis is performed on a one year simulation with a domestic load profile. This profile is generated by the software LoadProfileGenerator[6] and represents a yearly consumption of 5.4 MWh. Regarding the PV production, a yearly global horizontal irradiance (GHI) profile measured by NREL[7] is used to compute the generation profiles. The PV power profile is computed with (5).

$$P_{PV} = \frac{GHI \cdot P_{PV}^{peak}}{1000} \tag{5}$$

Where the PV peak power P_{PV}^{peak} is defined as the power produced by the PV installation under a GHI of 1000 W/m².

In the following, the PV installation production capacity is expressed throughout its self-sufficiency ratio (SSR). This parameter represents the ratio between the overall energy produced and the overall energy consumed over the period of interest and is linked to P_{PV}^{peak} with (6).

$$SSR = \frac{\int_{year} P_{PV} \cdot dt}{\int_{year} P_{load} \cdot dt} = \frac{\int_{year} GHI \cdot dt}{\int_{year} P_{load} \cdot dt \cdot 1000} \cdot P_{PV}^{peak} \tag{6}$$

The yearly operating cost is computed depending on the storage capacity and the SSR for optimally defined control strategy parameters. Indeed, these parameters are computed, for each storage capacity and SSR combination, using optimization algorithms in order to minimize the yearly operating cost. In other words, for given GHI and load consumption profiles and knowing the system model and the billing policy, the optimizer computes, for a set of storage capacity $\mathrm{C_{ss}}$ and SSR, the thresholds $\mathrm{E_0} - E_6$ and the power limitations P_{lim}^{inj} and P_{lim}^{ext} which minimize the yearly operating cost. This principle is illustrated in Figure 25.

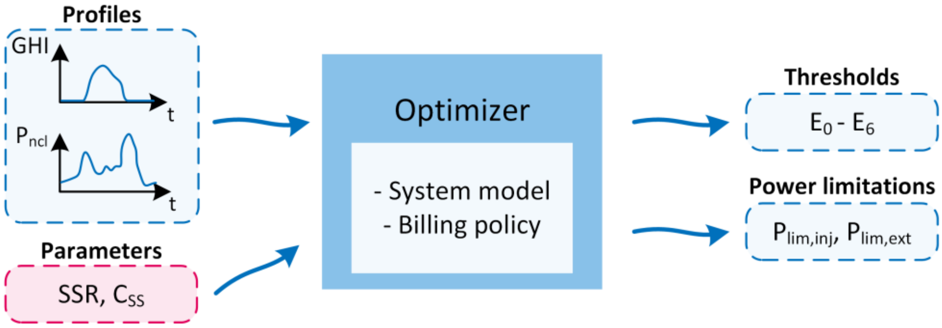

Figure 25: Control strategy parameters optimizer for economical assessment

[6] http://www.loadprofilegenerator.de/

[7] NREL, 'Oahu Solar Measurement Grid', *NREL*, 2011 <http://www.nrel.gov/midc/oahu_archive/> [accessed 30 March 2015].

To get relevant results, the economical assessment is made in comparison with a basic storage control strategy, which behaves in the following way:

- Store an excess of production until the storage is full,
- Supply a lack of production until the storage is empty.

Finally, the ESS is considered non-ideal during the whole economic analysis, with a fixed round-trip efficiency of 90%.

5.2 Impact of tariffs

First, the effect of the tariffs on the profitability is studied. The objective is to evaluate the influence of energy-based vs power-based cost components on the system profitability. The assessment is based on the billing rate from Viteos SA (DSO and energy provider of the city of Neuchâtel) for a low voltage grid connection "type B2"[8], which charges the energy as well as the maximum extracted power. In this category, two different tariffs, which will be compared, can be applied:

- B2A: with this tariff, the energy-based cost component is dominant
- B2B: with this tariff, the power-based cost component is dominant

The feed-in tariff used are the one applied by Viteos for a renewable energy source smaller than 30 kVA.[9]

For this first analysis, the cost of the storage system is neglected by assuming a LCOS null. This simplifying assumption allows to evaluate the impact of tariffs applied by the DSO only. Indeed, given the preponderant influence of current LCOS on the system profitability, taking into account this parameter would drown the cost difference attributable to the tariffs in the additional cost caused by the storage system.

In the next section, this simplifying assumption is eliminated and the impact of the storage cost is accurately assessed.

Figure 26 and Figure 27 represent the yearly operating cost difference, in CHF, between the DCSMART control system and a basic storage system, for both tariffs B2A and B2B, in function of the SSR and the storage capacity. A negative cost difference means that the DCSMART system is more profitable than a basic one with the same capacity.

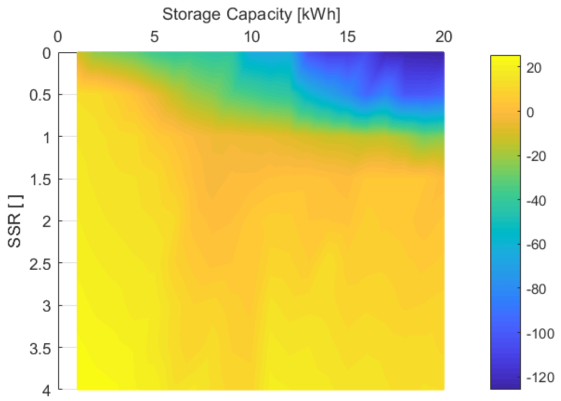

Figure 26: Difference in annual operating cost between the DCSMART and a standard storage system under tariff B2A

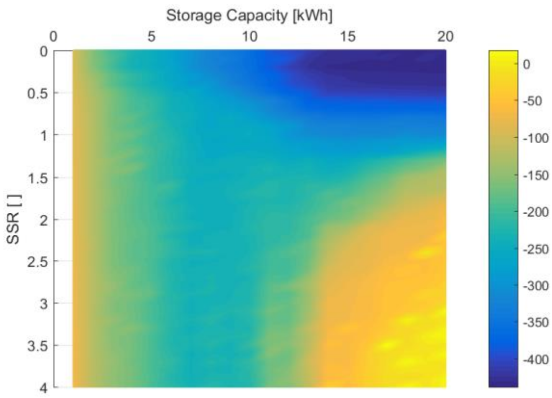

Figure 27: Difference in annual operating cost between the DCSMART and a standard storage system under tariff B2B

[8] https://www.viteos.ch/wp-content/uploads/2017/10/E_B2_2018_v1_1.pdf

[9] https://www.viteos.ch/wp-content/uploads/2017/10/E_ProductionERPC_2018_v1_1.pdf

These results first show that the performance of the DCSMART system is highly linked to the tariff applied, especially the cost of power. In Figure 26, the DCSMART system is mainly equivalent compared to a basic storage control strategy for a SSR higher than 1.5. In that situation, the peak-shaving is not profitable as the cost of power is not significant enough. Therefore, the whole storage capacity is used for self-consumption only. This kind of tariff obviously reduces the economical appeal of such a technology compared to a basic one.

However, the profitability is real and significant when the applied tariff puts the emphasis on the cost of the power. As an example, it can be observed in Figure 27, for a realistic setup with a storage capacity of 8 kWh and a SSR of 2.5, a saving of CHF 240 (namely 16%) compared to a basic storage system. This figure also shows that the system is profitable in most of the situation for tariff B2B. This is mainly linked to the performed power limitation which allows significant savings regarding the consumed power. In that case, the potential of multi-services provided by DCSMART is fully exploited. It can be deduced that such a system is particularly useful for applications characterized by important power peaks, even more so that the power-related component of the electricity bill is bound to increase due to increasing number of prosumers in Switzerland.

5.3 Impact of LCOS

The second analysed aspect is the effect of the levelized cost of storage (LCOS) on the system profitability. For this assessment, the following setup is evaluated:

- Storage capacity = 8kWh
- SSR = 2.5
- Tariff = B2B
- Yearly consumption = 5.4MWh

As mentioned above, the LCOS accounts for the cost of the storage system and its lifespan. It is defined as the total lifetime cost of an investment divided by the cumulated energy stored by this investment. It thus represents the cost linked to the storage of a given amount of energy and is expressed in CHF/kWh. It is computed in the following way:

$$LCOS = \frac{I_{SS}}{C_{SS} \cdot N_{cycle} \cdot \eta_{rt} \cdot DoD} + Ancillary\ Cost \quad (6)$$

where I_{SS} is the total investment cost, C_{SS} the storage capacity, N_{cycle} the number of cycle, η_{rt} the round-trip efficiency and DoD the allowed depth of discharge.

The analysis is made for a LCOS varying between 0.05 to 0.25CHF/kWh, which represents a realistic range for current and upcoming LCOS. Indeed, according to [6], the LCOS for automotive batteries is evaluated at 0.15€/kWh (0.18CHF/kWh) in 2015 and expected to fall down to 0.05€/kWh (0.06CHF/kWh) in 2030. Figure 28 depicts an estimation and projection of the battery and storage cost for automotive batteries.

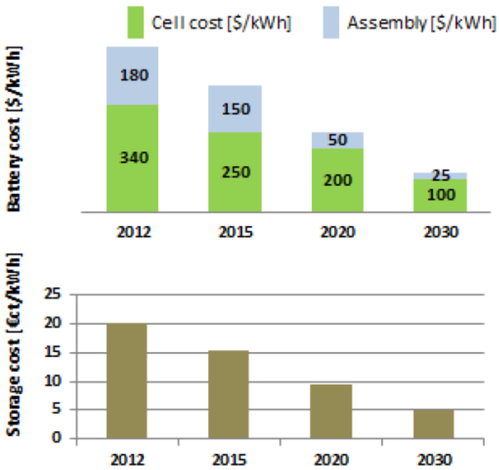

Figure 28: (upper part) LIB cost development for automotive (EV) batteries, both for cell and packaging cost; (lower part) development for estimated storage cost per kWh.[10]

W. Hoffmann states[11] that this cost decrease is directly linked to the cumulative installed capacity, similarly as it can be observed in a number of mass products like semiconductor storage chips, flat panel displays and photovoltaic modules.

Table 7 summarizes the relative savings achieved by DCSMART and a basic storage compared to a system without storage in function of the LCOS, using tariff B2B.

Table 7: Effect of LCOS

LCOS [CHF/kWh]	Savings DCSMART compared to no storage [%]	Savings basic storage compared to no storage [%]
0	20.0	5.2
0.05	13.3	-3.6
0.10	6.4	-12.4
0.15	2.7	-21.1
0.20	-2.1	-29.9
0.25	-7.6	-38.7

The first observation which can be made is the poor profitability of a basic system when taking into account a non-zero LCOS. Indeed, the system becomes profitable only for LCOS below 5ct/kWh. Knowing the feed-in tariff currently applied by Viteos SA (12ct./kWh), it is easily understandable to observe such results. If the difference between the energy buying tariff and feed-in tariff is lower than the LCOS, it is therefore less expensive to feed an excess of production back to the grid instead of storing it locally for a later consumption. In other words, it is currently not profitable to use a storage system to increase self-consumption only.

---

[10] W. Hoffmann, 'Importance and Evidence for Cost Effective Electricity Storage' (presented at the 29th European Photovoltaic Solar Energy Conference and Exhibition, Amsterdam, The Netherlands, 2014) <http://www.eupvsec-proceedings.com/proceedings?paper=31772> [accessed 2 February 2015].

[11] Hoffmann, 'Importance and Evidence for Cost Effective Electricity Storage'.

What is interesting to notice is that the DCSMART system becomes already profitable for a LCOS of 15ct./kWh, namely 10ct./kWh before a basic control storage. It is able to achieve such performance by making the most of its capability in providing multiple services. It can be observed that profitability is drastically increased by limiting the consumed power in addition to self-consumption. Although such a system is not profitable with today's LCOS, it is expected to become profitable sooner and in a greater extent than a basic storage system. Beyond that, the service of ramp-rate alleviation (RRA) performed by DCSMART, which has for the time being no economic value despite its undeniable technical benefits on the power quality (PQ), could increase even more strongly the system profitability. Indeed, future billing policies are predicted to value more this aspect e.g., by introducing PQ markets as an incentive to efficiently achieve the required levels of PQ.[12]

5.4 Analysis on the predefined load profiles

To conclude this economical assessment, a similar analysis is performed using the characteristic consumption profiles defined in Section 3.5.1. For that assessment, these daily load profiles are repeated over the whole year.

The same setup as in the previous section is used, i.e. $C_{ss} = 8kWh$, $\mathrm{SSR} = 2.5$ and $\mathrm{tariff} = B2B$. As for the first analysis, the simplifying assumption of a LCOS null is made in order to focus the assessment on the impact of the load profile. To have comparable results, the scale of the load profiles have been adapted to get a yearly consumption equal to 5.4 MWh. That way, it is possible to compare the impact of the shape of the load profiles.

Table 8 gathers the yearly operating cost for the three reference profiles in the case of a system without storage, with a DCSMART storage and with a basic storage. The relative difference with respect to the reference (system without storage) is written in brackets. As a reminder, the reference profile #1 is the most constant and reference profile #3 is the most variable.

Table 8: Yearly cost analysis for predefined load profiles

Reference Profile	No Storage (ref) [CHF]	DCSMART [CHF]	Basic Storage [CHF]
1	1091	1094 (+0.3%)	1096 (+0.5%)
2	1144	1095 (-4.3%)	1136 (-0.6%)
3	1283	1114 (-13.2%)	1243 (-3.1%)

With this analysis of the first reference load profile, it can be observed that, even with a LCOS equal to zero, having a storage system to increase self-consumption or perform peak-shaving is not necessarily profitable. This is caused by the fact that the storage system is modeled with a 90% round-trip efficiency. Therefore, 10% of the stored energy is lost which obviously has a negative impact on the system profitability. For flat consumption profiles, no economic advantages are observed when installing such a system. The consideration of the consumption profile shape is therefore essential in the design process. This last statement underline the usefulness of the analysing tools developed in the scope of this project.

Having a high variability in the consumed power is however much more favourable towards installing a buffering storage system to decrease operating cost. The results obtained with reference profile #3 are consistent with those observed until now. Indeed, in that situation, the DCSMART storage demonstrates a higher profitability compared to a

[12] Bossche, Meersman and Vandevelde, 'Fundamental Tarification of Electricity', 1–7.

basic storage due to its ability to perform additional services, in particular power limitation.

6. Conclusion

The most important thing to keep in mind from this economic assessment is that the profitability of a buffering storage system is highly dependent on:

- the applied tariffs, in particular
    - the cost of the power
    - the feed-in retribution
- the LCOS
- the shape of the load consumption

Regarding the first element, it has been shown that the higher the power cost, the higher the profitability of the DCSMART system. As mentioned earlier, billing policies are expected to tend towards an increase of the power-related component of the electricity bill. This predicted trend would lead to an increase of the DCSMART system profitability.

The LCOS is also determining for the buffering storage system profitability. It has been showed that with the current LCOS, such systems are not yet profitable. But with the expected drop of the LCOS, their profitability will increase. Results showed that this rate of increase is way higher for the DCSMART system than for a basic system.

The last aspect is linked to the very own nature of the consumer, the shape of the load consumption. Results have shown that no benefit are brought by a buffering storage system in the case of a flat power consumption. However, the higher the consumption variation, the higher the profitability of such a system. This profitability is, once again, higher for the DCSMART system compared to the basic one.

All these elements show that, despite not being economically profitable for the time being, the DCSMART system is expected to become profitable in the near future. This is expected to happen faster and in a greater extent compared to a basic system.